Since January 2020 Elsevier has created a COVID-19 resource centre with free information in English and Mandarin on the novel coronavirus COVID-19. The COVID-19 resource centre is hosted on Elsevier Connect, the company's public news and information website.

Building and Environment 234 (2023) 109967

Contents lists available at ScienceDirect

Building and Environment

journal homepage: www.elsevier.com/locate/buildenv

Safe CO_2 threshold limits for indoor long-range airborne transmission control of COVID-19

Xiaowei Lyu [a], Zhiwen Luo [b,*], Li Shao [a], Hazim Awbi [a], Samuele Lo Piano [a]

[a] School of the Built Environment, University of Reading, UK
[b] Welsh School of Architecture, Cardiff University, UK

ARTICLE INFO

Keywords:
Infection risk control
CO_2 monitoring
Initial quanta
Uncertainty analysis

ABSTRACT

CO_2-based infection risk monitoring is highly recommended during the current COVID-19 pandemic. However, the CO_2 monitoring thresholds proposed in the literature are mainly for spaces with fixed occupants. Determining CO_2 threshold is challenging in spaces with changing occupancy due to the co-existence of quanta and CO_2 remaining from previous occupants. Here, we propose a new calculation framework for deriving safe excess CO_2 thresholds (above outdoor level), C_t, for various spaces with fixed/changing occupancy and analyze the uncertainty involved. We categorized common indoor spaces into three scenarios based on their occupancy conditions, e.g., fixed or varying infection ratios (infectors/occupants). We proved that the rebreathed fraction-based model can be applied directly for deriving C_t in the case of a fixed infection ratio (Scenario 1 and Scenario 2). In the case of varying infection ratios (Scenario 3), C_t derivation must follow the general calculation framework due to the existence of initial quanta/excess CO_2. Otherwise, C_t can be significantly biased (e.g., 260 ppm) when the infection ratio varies greatly. C_t can vary significantly based on specific space factors such as occupant number, physical activity, and community prevalence, e.g., 7 ppm for gym and 890 ppm for lecture hall, indicating C_t must be determined on a case-by-case basis. An uncertainty of up to 6 orders of magnitude for C_t was found for all cases due to uncertainty in emissions of quanta and CO_2, thus emphasizing the role of accurate emissions data in determining C_t.

1. Introduction

COVID-19, as a novel coronavirus disease, has caused a worldwide pandemic since the end of 2019 [1]. Indoor transmission control is crucial in preventing the spread of the SARs-CoV-2 due to a higher transmission risk indoors than outdoors [2]. The four main transmission routes in indoor environments are droplet-borne, fomite, short-range airborne, and long-range airborne [3,4]. While short-range airborne transmission route was inferred to be the dominant route in close contact [1], long-range airborne transmission was revealed to more likely induce outbreaks in poorly ventilated and confined indoor spaces [5]. Thus, it is of primary importance to monitor and control long-range airborne transmission in indoor environments.

The exhaled infectious aerosols contributing to long-range airborne transmission are difficult to be detected. Hence, there is an urgent need for a detectable indicator to effectively monitor long-range airborne transmission. CO_2, which can be easily monitored through low-cost sensors [6], has been recommended because it can both reflect the indoor ventilation condition and the quanta concentration [7]. Accordingly, safe CO_2 thresholds are defined as the maximum CO_2 concentration level under which the indoor space is at an acceptable infection risk level. Such information is useful in guiding the design of infection-resilient buildings.

Treating CO_2 as an indicator for indoor ventilation performance, recent studies proposed CO_2 thresholds for risk control based on prevailing ventilation standards aimed at ensuring acceptable indoor air quality (IAQ) but not infection risk [8–10]. Although ASHRAE does not recommend a specific value of threshold [7], other organizations have suggested specific CO_2 thresholds of 800 ppm [11,12] or 800–1000 ppm [8] to ensure a safe indoor environment. However, it is questionable whether a fixed CO_2 threshold can guarantee a low infection risk for all spaces, as factors such as occupancy level and respiratory activity can all affect the value of it [6].

Moving beyond using CO_2 as a mere indicator of indoor ventilation condition, CO_2 can also be used to directly reflect quanta concentration as CO_2 and virus-laden aerosols are co-produced and co-inhaled by human. In this context, CO_2 thresholds can be calculated backward

* Corresponding author.
E-mail address: LuoZ18@Cardiff.ac.uk (Z. Luo).

https://doi.org/10.1016/j.buildenv.2022.109967
Received 15 October 2022; Received in revised form 16 December 2022; Accepted 29 December 2022
Available online 30 December 2022

Nomenclature

B	Breathing rate, m^3/h
$C_{CO2,i}$	CO_2 concentration for occupancy stage i, ppm
$C_{Cin,i}$	Initial CO_2 concentration for occupancy stage i, ppm
$C_{q,i}$	Quanta concentration for occupancy stage i, quanta/m^3
$C_{qin,i}$	Initial quanta concentration for occupancy stage i, quanta/m^3
C_t	Safe excess CO_2 threshold, ppm
C_{t50}	Median safe excess CO_2 threshold, ppm
E_{CO2}	CO_2 emission rate, mL/s
E_q	Quanta emission rate, quanta/h
I_i	Infector number for occupancy stage i
N_{ave}	Average occupant number
N_i	Occupant number for occupancy stage i
P_i	Infection risk for occupancy stage i
P_t	Predefined infection risk threshold
P_I	Community prevalence
R_A	The average number of secondary cases caused by one infector
S_i	Occupancy stage i
T_i	Exposure time for occupancy stage i, h
V	Space volume, m^3
λ_i	Air change rate for occupancy stage i, h^{-1}

based on a pre-defined acceptable infection risk level [6,13]. Indoor airborne transmission risk is constrained under the predefined risk level in as much indoor CO_2 concentration is maintained below the derived threshold. Occupancy level and respiratory activity for a particular indoor space can all be factored in this backward calculation process [6,13,14]. In the literature of using CO_2 to reflect quanta concentration, the derived thresholds were found to be highly sensitive to factors such as activity level and community prevalence, making CO_2 thresholds vary across different indoor spaces [6]. For example, the reference excess CO_2 threshold (above outdoor level) for a classroom amounts to only about 150 ppm, while this figure is ten-fold for a supermarket [6]. This indicates that the CO_2 thresholds should be determined case by case, instead of using a fixed value for all spaces.

In addition, most proposed thresholds are for spaces with fixed occupancy level under the assumption of no initial quanta/excess CO_2 [6,13,14]. For spaces with varying occupancy, some of quanta/CO_2 released by earlier occupants can remain in the space and become initial quanta/CO_2 when the next group occupies the space, potentially increase the infection risk. The quantity of initial quanta is essential for defining CO_2 threshold, but it is difficult to estimate, as it requires information about ventilation conditions and occupancy profile of previous occupants. Hence, how can we account for initial quanta/excess CO_2 in spaces with changing occupancy in infection risk assessment remains an unsolved question [3,15].

Finally, emissions of quanta and CO_2 are crucial in determining the CO_2 threshold. However, they both exhibit inter-individual variability and can be affected by factors such as age and gender [16–18]. For instance, the viral load of a super-spreader can be 10 times higher than the mean level of normal infectious subjects [19], indicating a higher quanta emission [20,21]. Different values of quanta and CO_2 emission were adopted by previous studies for CO_2 threshold derivation, e.g., from 0.37 quanta/h to 100 quanta/h for classrooms [6,13,16,22]. The effect of the uncertainty in the emissions of quanta and CO_2 on CO_2 threshold needs further investigation. The present study aims to provide a new calculation framework for deriving safe excess CO_2 thresholds (C_t) by taking into account initial quanta/excess CO_2 and changing/fixed occupancy patterns in different indoor spaces, as well as propagating the uncertainty of these input variables.

2. Methodology

2.1. General calculation framework

Our model is based on four assumptions for indoor mass balance equations for CO_2 and quanta [13]: 1) both CO_2 and quanta are well mixed and evenly distributed in the air; 2) indoor excess CO_2 is released only by human exhalation, with no other indoor sources; 3) CO_2 emission rate and quanta emission rate are both constant (i.e., not time dependent); 4) the loss of quanta is mainly due to ventilation, other elimination mechanisms such as deposition, filtration and inactivation are neglected.

In deriving C_t for spaces with changing occupants, we consider a sequence of occupancy stages, S_i (I_i, N_i, T_i). Stage i represents an indoor space (with the volume of V)being occupied by a number of occupants (N_i) with infectors (I_i) for a duration of time (T_i). $i = 1$ represents the start of the occupancy: N_1 occupants (with I_1 infectors) stay in this indoor space for a period of T_1, with no people inside prior to N_1 occupants. The introduction of various occupancy stages aims to consider the virus released and still present in the air from previous occupancy stages (the initial quanta). This is fundamentally different from previous studies which only considered one-off occupancy or fixed occupancy throughout the exposure period of interest.

The general calculation process of C_t for one occupancy stage of a space is given as follows.

Long-range transmission risk for occupancy stage i is modeled through a Wells-Riley model [23] amended by Gammitoni and Nucci [24] to assess infection risk through unsteady-state quanta concentration:

$$P_i = 1 - e^{-B\int_0^{T_i} C_{q,i}(t)dt} \tag{1}$$

Quanta concentration in Equation (1) is modeled through transient mass balance equation:

$$\frac{dC_{q,i}}{dt} = \frac{I_i E_q}{V} - \lambda_i C_{q,i} \tag{2}$$

Equation (2) can be analytically solved as:

$$C_{q,i}(t) = \left(C_{qin,i} - \frac{I_i E_q}{\lambda_i V}\right) e^{-\lambda_i t} + \frac{I_i E_q}{\lambda_i V} \tag{3}$$

To control transmission risk of stage i under an acceptable low level, a risk threshold of P_t needs to be initially determined. Based on P_t, a required ACH (air change rate, λ_i) can be derived by substituting Equation (3) into Equation (1), λ_i should be no less than the derived value to keep transmission risk under P_t.

Indoor excess CO_2 concentration is also dominated by ACH, hence it reflects the ventilation condition of stage i.

Indoor excess CO_2 concentration for stage i is modeled by mass balance equation (4):

$$\frac{dC_{CO2,i}}{dt} = \frac{N_i E_{CO2}}{V} - \lambda_i C_{CO2,i} \tag{4}$$

Equation (4) is solved as:

$$C_{CO2,i}(t) = \left(C_{Cin,i} - \frac{N_i E_{CO2}}{\lambda_i V}\right) e^{-\lambda_i t} + \frac{N_i E_{CO2}}{\lambda_i V} \tag{5}$$

Substituting the required ACH that is backward calculated from transmission risk threshold into Equation (5), the time-averaged indoor excess CO_2 concentration ($C_{CO2,i}$) during T_i is exactly C_t for stage i [13,22]:

$$C_t = \frac{1}{T_i}\int_0^{T_i} C_{CO2,i}(t)dt \tag{6}$$

When indoor excess CO_2 concentration is below the reference threshold C_t, it indicates that there is sufficient ventilation to keep long-

range transmission risk for occupancy stage i under the risk level of P_t.

For different occupancy stages, C_t can be derived by following the steps described above, taking into account the existence of initial quanta/excess CO_2, see Equation (3) and Equation (5). Starting with occupancy stage 1, which has no initial quanta/excess CO_2,the required ACH (λ_1) can be easily obtained following the general calculation process. For occupancy stage 2, the initial quanta and initial excess CO_2 can be estimated based on the ACH derived for occupancy stage 1 (λ_1), under the assumption that excess CO_2 during occupancy stage 1 has been controlled below the reference threshold, C_t for occupancy stage 2 can then be calculated according to the calculation framework. This process can be repeated for all the modeled occupancy stages by using the ACH derived from the previous occupancy stages to estimate the initial quanta/excess CO_2 for the current stage, and thereby calculating C_t iteratively.

2.1.1. Infection risk threshold P_t

The infection risk threshold, P_t, is crucial in determining the safety levels of the indoor environment. It can be defined in two ways, either by using a constant value for all environments, such as 1%, 0.1% [25] or even 0.01% [6], or by determining P_t based on the reproductive number (R_A) where R_A is the average number of secondary cases caused by one infector in a given susceptible population in indoor environment. In the latter, the value of P_t is determined by the number of occupants and can become a large and inconvincible value when occupant number is small [26,27]. In this study, we use a constant value of $P_t = 0.01\%$ as suggested by Peng and Jimenez [6], which is reasonable for most occupancy stages when the number of occupants is less than 10,000.

2.2. Designed scenarios

Three scenarios were identified to calculate C_t.

1) Regularly attended space with fixed occupancy level and the same group of people as occupants, so that $N_1 = N_2 = \ldots$ (e.g., a lecture room used by a certain group of students) [28,29];
2) Non-regularly attended space with constant infection ratio ($I_1/N_1 = I_2/N_2 = \ldots = I_i/N_i$), different groups of people as occupants, and a high occupancy level (e.g., shopping center, train station);
3) Non-regularly attended space with changing infection ratios ($I_1/N_1 \neq I_2/N_2 \neq \ldots \neq I_i/N_i$) and low occupancy level (e.g., gym, train coach).

All these scenarios are widely experienced in real-life situations.

2.2.1. Scenario 1: regularly attended spaces

We determined the number of infectors I_i for Scenario 1 based on both the indoor occupancy level (N_i) and local community prevalence (P_I). The expected I_i is defined as max {1, $P_I N_i$}. When with a low indoor occupancy level or a low community prevalence, the value of $P_I N_i$ can be less than 1. In such case, I_i was assumed to be equal to 1. Otherwise, I_i was assumed to be $P_I N_i$ to reflect the real local infection condition.

Quanta concentration and excess CO_2 concentration were found to have a constant proportion throughout all the occupancy stages, as determined from the mass balance equations. This proportion was only affected by infection ratio and emissions, see Equation (7) (Full derivation details can be found in Supplementary Information). As long as the infection ratios and emissions remained unchanged during the occupancy stages, the proportion remains unchanged as well, hence:

$$\frac{C_{q,1}(t)}{C_{CO2,1}(t)} = \frac{C_{q,2}(t)}{C_{CO2,2}(t)} = \ldots = \frac{I_i}{N_i}\frac{E_q}{E_{CO2}} \tag{7}$$

Under these circumstances, infection risk for stage i in Eq (1) can be revised as below:

$$P_i = 1 - e^{-B\frac{I_i}{N_i}\frac{E_q}{E_{CO2}}\int_0^{T_i} C_{CO2,i}(t)dt} \tag{8}$$

Equation (8) can be treated as the classical rebreathed fraction (RF)-based infection risk model derived by Rudnick and Milton [14], with $BC_{CO2,i}/E_{CO2}$ representing the rebreathed fraction. This derivation proved that rebreathed fraction (RF)-based model can account for the impact of initial quanta/excess CO_2 in risk assessments for spaces with fixed occupants.

Based on Equation (8), the time averaged value C_t for occupancy stage i can then be derived as:

$$C_t = \frac{E_{CO2}N_i}{E_q T_i B I_i} ln\left(\frac{1}{1-P_t}\right) \tag{9}$$

2.2.2. Scenario 2: Non-regularly attended spaces with constant infection ratios

In Scenario 2, we assumed that community prevalence (P_I) can directly represent indoor infection ratio due to the high occupancy level ($I_1/N_1 = I_2/N_2 = \ldots = P_I$). The proportion between $C_{q,i}$ and $C_{CO2,i}$ also becomes constant due to the constant infection ratio among occupancy stages (Detailed derivation process can be found in Supplementary Information):

$$\frac{C_{q,1}(t)}{C_{CO2,1}(t)} = \frac{C_{q,2}(t)}{C_{CO2,2}(t)} = \ldots = P_I\frac{E_q}{E_{CO2}} \tag{10}$$

Similar as Scenario 1, the infection risk and excess CO_2 threshold can then be derived as:

$$P_i = 1 - e^{-BP_I\frac{E_q}{E_{CO2}}\int_0^{T_i} C_{CO2}(t)dt} \tag{11}$$

$$C_t = \frac{E_{CO2}}{E_q T_i B P_I} ln\left(\frac{1}{1-P_t}\right) \tag{12}$$

Equation (11) can be treated as an extension of the classical RF-based infection risk model. The generality of the original model is extended from scenarios with fixed occupants (scenario 1) to scenarios with varying occupancy levels (scenario 2), taking into account initial quanta/excess CO_2. It should be noted that T_i in Scenario 2 is often difficult to monitor, as the occupancy level keeps changing. An alternative method is to predefine it based on the characteristics of different spaces. For example, T_i could be set as 35 min for check-in hall and 100 min for departure hall, based on the average dwelling times measured in an airport [30].

2.2.3. Scenario 3: Non-regularly attended spaces with changing infection ratios

In Scenario 3, the indoor infection ratio cannot be represented by P_I due to the relatively low occupancy level. To ensure a safe indoor environment, it is recommended to use the maximum value of {1, $P_I N_i$} to determine the number of infectors (I_i), as was done in Scenario 1. In these circumstances, the infection ratio will change among the occupancy stages, and quanta concentration cannot be represented by excess CO_2 concentration. C_t derivation must follow the general calculation process (see Part 2.1).

It should be noted that the general calculation process does not require the field measurement of ACH and instead relies on a known occupancy profile, including the number of occupants and the duration of occupancy for all the occupancy stages. Thus, this method may be more suitable for spaces in Scenario 3 where the occupancy profile (N_i and T_i) of each occupancy stage can be monitored simultaneously or obtained before the spaces being occupied, such as the rail train or theatre.

2.3. Uncertainty analysis and inputs

An uncertainty analysis was carried out considering E_q and E_{CO2} have interindividual variations and can vary with gender and age, leading uncertainty to C_t. The probability density functions (PDF) of E_q for three

different activities were obtained from recent research by Buonanno et al. [16], where they found the quanta emissions follow a log10-normal distribution, see Table 1. E_{CO2} was also assumed to be lognormally distributed with a standard deviation equal to 20% of its mean [31]. The mean value for the distribution was calculated as the average value of E_{CO2} of female and male individuals aged 30–40 years (the most frequent age cohort), and with a specific metabolic equivalent [17]. The metabolic equivalent for E_{CO2} was specified by different activity levels, specifically, 1.5 met for sedentary activity, 3 met for light activity and 9 met for heavy activity [32]. Latin Hypercube sampling (LHS) [33] was used to generate a total of 30,000 samples from emissions of quanta and CO_2, due to its advantage in accurately reflecting the underlying distribution of inputs with a smaller sample size. Monte Carlo simulations [34] were used to propagate and quantify the uncertainty in predictions.

Typical indoor environments were selected for each scenario based on factors such as occupancy level, infection ratio, etc. (Tables 2 and 3). Cases in Scenario 1 have a fixed but different number of occupants, recognizing that occupant number is a dominant parameter in deriving C_t in Scenario 1, see Equation (9). It should be noted that lecture hall case in Scenario 1 has 3 infectors because of its high occupancy level, while other cases have only 1 infector due to the relatively low occupancy level. In Scenario 2 a shopping center was selected as the case study with variable levels of community prevalence, which were adopted from three different COVID-19 periods in the UK in 2020 [35] to represent relatively small (0.06%), median (0.4%) and high (1%) community prevalence levels. The highest level of community prevalence was adopted for Scenario 1 and Scenario 3. Two cases with low and changing occupancy levels were selected for Scenario 3 (i.e., a train coach and a gym room). As regards occupancy stages, only one stage was included for cases in Scenario 1 and Scenario 2, whereas five occupancy stages were included for cases in Scenario 3 to take into account the variability in C_t resulting from the impact of initial quanta/excess CO_2. Different categories of activities were considered in the cases of the different scenarios. Cases in Scenario 1 were assumed to have "sedentary activity - breathing", which is typical for people sitting or standing in office or classroom environments. Cases in Scenario 2 are assumed to have "light activity - speaking", as people are usually walking in the shopping center and talking to each other. For scenario 3, two activities were included to explore the effects of activity level on C_t determination, specifically, "sedentary activity – breathing" for the train coach and "moderate activity – breathing" for gym. The breathing rates (B) corresponding to different physical activity levels were adopted from previous research [36].

3. Results

3.1. Safety excess CO_2 threshold varies in different scenarios

For Scenario 1, the number of occupants (N_i) is the dominant factor that affects C_t and scales with it (see Equation (9)). C_t for cases occupied by different N_i in Scenario 1 (regularly attended spaces) have substantial differences, see Fig. 1(a). The highest C_{t50} (the median value of C_t) occurs in lecture hall (890 ppm), followed by lecture classroom (580 ppm), classroom (270 ppm), the lowest one is in office environment (180 ppm), although significant overlaps exist in the output distributions (Fig. 1(a)).

For Scenario 2, instead of N_i, C_t is dominated by community prevalence (P_I), as C_t is inversely proportional to P_I (see Equation (12)). Three different values of P_I (i.e., 0.06%. 0.4% and 1%) were adopted to derive C_t and the results are showed in Fig. 1(b). The highest C_{t50} of 870 ppm refers to the lowest P_I of 0.06%, and the lowest C_{t50} of 50 ppm to the highest P_I of 1%.

For Scenario 3, the changing infection ratios lead to different values of C_t for different occupancy stages. For train coach, C_{t50} are approx. 180 ppm, 320 ppm, 650 ppm, 410 ppm and 200 ppm corresponding to infection ratios of 1/20, 1/40, 1/80, 1/40 and 1/20 for the five stages in sequence, while they are 7 ppm, 15 ppm, 30 ppm, 15 ppm and 7 ppm for gym environment corresponding to infection ratios of 1/5, 1/10, 1/20, 1/10 and 1/5. The changing infection ratios can lead to different C_t values in different stages mainly because the existence of initial quanta/excess CO_2. For instance, if initial quanta/excess CO_2 is not considered, C_{t50} for Stage 2 and Stage 4 of train coach with the same occupant number should be same, but the difference of C_{t50} between the two occupancy stages reaches approx. 80 ppm due to the impact of initial quanta/excess CO_2.

Furthermore, the general cases in Scenario 3 also demonstrate that the activity level is another major factor that can affect the derived thresholds, see Fig. 1(c). C_t for gym with a high activity level is much lower than that for train coach with a sedentary activity level due to the relative high activity level in gym environment (hence, high emission rate for quanta). This agrees with previous studies [37,38] that there should be much higher restrictions in spaces with high activities such as gym to control airborne infection risk.

Apart from the substantially different C_t among different cases, large uncertainty of C_t was also observed in each case, spanning up to six orders of magnitude on a log scale (see Fig. 1). Fig. 1 shows that cases with a large median value contain more uncertainty, as seen in the right-shifted log-scaled distribution of C_t, indicating that C_t can be more affected by the uncertainty of emission settings considered in our study. Given the large uncertainty of C_t and the non-normal distribution when transformed to a linear scale, the median safe excess CO_2 threshold (C_{t50}) is an appropriate descriptive statistic for excess CO_2 threshold, due to its high probability density [39].

3.2. Effect of infection risk threshold (P_t)

As discussed before, the infection risk threshold (P_t) plays a role in deriving C_t. Different P_t have been adopted in different research in the range of 0.01%–1% [6,25,40,41]. Here we explore how P_t will affect C_t with results shown in Fig. 2. The base case is the classroom in Scenario 1 (see Table 2). C_{t50} is found to be approximately linearly related to P_t with approx. 270 ppm for $P_t = 0.01\%$ to 27000 ppm for $P_t = 1\%$, which reveals the high sensitivity of C_{t50} to P_t.

3.3. Effect of initial conditions

We have shown that initial condition of quanta and excess CO_2 can affect the derived safe excess CO_2 threshold when infection ratio varies among the occupancy stages. However, most previous studies have neglected the consideration of the initial conditions of quanta and excess CO_2 in C_t derivation [6,13,14]. To further quantify the impact of initial condition of quanta/excess CO_2 on C_t when infection ratio varies, we compared two cases: 1) with initial quanta/excess CO_2; 2) without them. We assumed the two cases with the same indoor volume of 300 m^3, both occupied with two stages. The occupants in both cases were assumed to have "sedentary activity – breathing", and only one infector is included.

In case 1, 20 occupants were assumed to be present in Stage 1, and the number of occupants in Stage 2 changes to 5, 10, 20, 40, 80 respectively. This means the infection ratio will change from 1/20 (Stage 1) to 1/5, 1/10, 1/20, 1/40, 1/80 (Stage 2) accordingly, and initial quanta and excess CO_2 can affect C_t in Stage 2 to varying degrees.

Table 1
Inputs for Uncertainty Analysis. Distribution mean and standard deviation in brackets.

Activity	Quanta emission PDF (quanta/h)	CO_2 emission PDF (mL/s)
Sedentary - breathing	LN10 (−0.429, 0.720)	LN (5.05, 1.01)
Light activity - speaking	LN10 (0.698, 0.720)	LN (10.10, 2.02)
Heavy activity - breathing	LN10 (0.399, 0.720)	LN (34.20, 6.84)

Table 2
Inputs of uncertainty analysis for Scenario 1 and Scenario 2.

Case	Volume (m^3)	Infector number	Occupant number	Exposure time (h)	Community prevalence	Breathing rate (m^3/h)
Scenario 1						
Classroom	231	1	30	1	1%	0.54
Lecture classroom	270	1	65	1	1%	0.54
Lecture hall	540	3	300	1	1%	0.54
Open-plan office	594	1	20	1	1%	0.54
Scenario 2						
Shopping center	2040	–	–	1	0.06%, 0.4%, 1%	1.38

Table 3
Inputs of uncertainty analysis for Scenario 3.

Scenario 3	Stage 1	Stage 2	Stage 3	Stage 4	Stage 5
Train coach (300 m^3)					
Infector number	1	1	1	1	1
Occupant number	20	40	80	40	20
Exposure time (h)	1	1	1	1	1
Community prevalence	1%	1%	1%	1%	1%
Breathing rate (m^3/h)	0.54	0.54	0.54	0.54	0.54
Gym (600 m^3)					
Infector number	1	1	1	1	1
Occupant number	5	10	20	10	5
Exposure time (h)	1	1	1	1	1
Community prevalence	1%	1%	1%	1%	1%
Breathing rate (m^3/h)	3.30	3.30	3.30	3.30	3.30

In case 2, no occupants were assumed to be present in Stage 1 (hence, no initial quanta/excess CO_2), and 5 different occupancy levels were assumed for Stage 2, similar to case 1. Our aim is to derive C_t for Stage 2 for both cases with consideration of the impacts of initial quanta and excess CO_2 from Stage 1 (case 1) and without (case 2). The differences between the results of two cases can be used to quantify the impact of initial quanta and excess CO_2 on C_t. It is straightforward to derive C_t for case 2, as there are no initial quanta and excess CO_2, while for case 1, an estimation of initial quanta/excess CO_2 is necessary. Considering the excess CO_2 concentration is affected by different factors such as exposure time and ACH during Stage 1, we assumed a constant value for initial excess CO_2 concentration for Stage 2 in case 1, namely 1000 ppm. The initial quanta can then be derived based on this value and the infection ratio of Stage 1 (see Eq. S4 in Supplementary).

Fig. 3 shows the derived C_t value of case 1 with initial quanta/excess

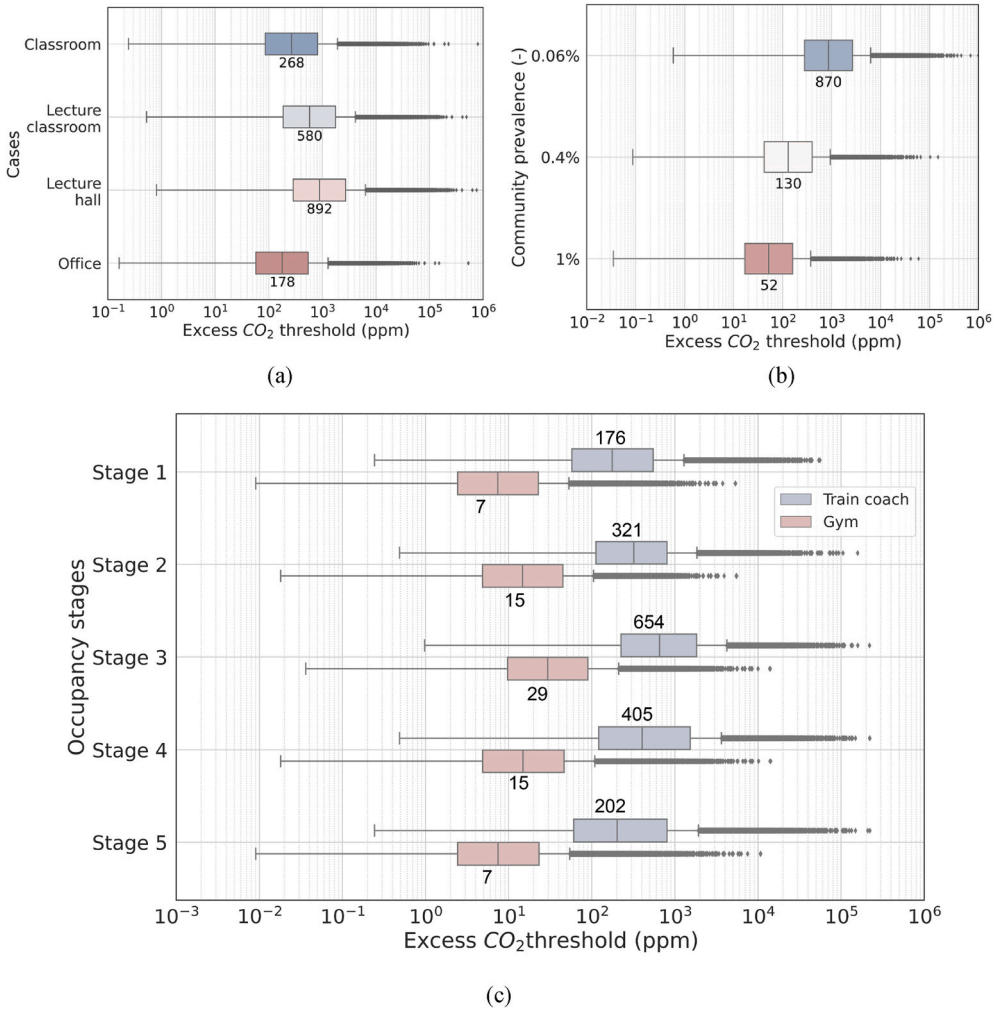

Fig. 1. Safe excess CO_2 thresholds for 3 scenarios: (a) Scenario 1(with fixed occupancy); (b) Scenario 2 (with changing occupancy but fixed infection ratios); (c) Scenario 3 (with changing occupancy and changing infection ratios).

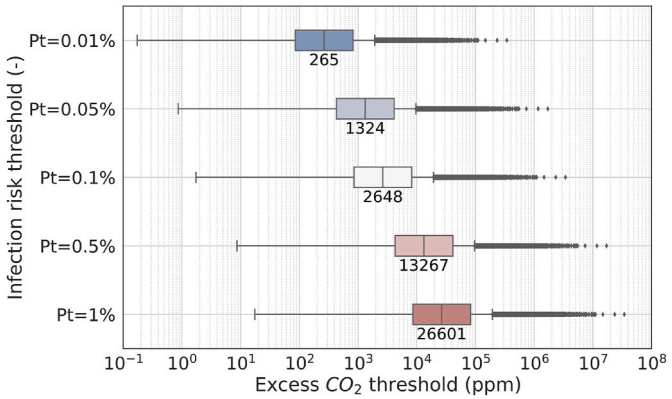

Fig. 2. Excess CO_2 thresholds for the classroom (see Table 2) under different infection risk thresholds.

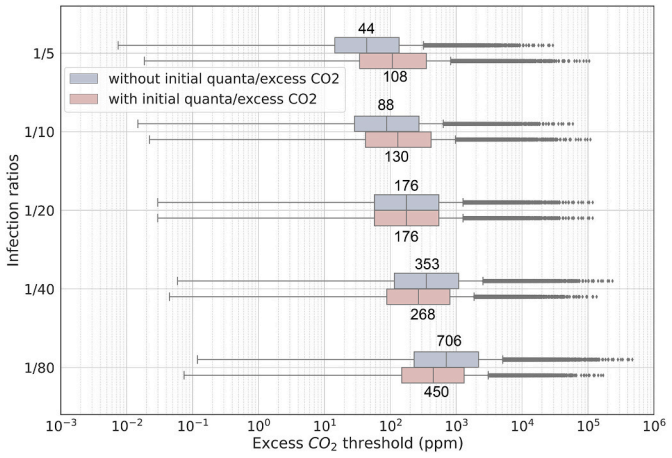

Fig. 3. Excess CO_2 threshold of the second occupancy stage of an indoor space (300 m^3) under different infection ratios considering with and without initial quanta/excess CO_2.

CO_2 has distinct difference from that of case 2 without initial quanta/excess CO_2, when its infection ratio in Stage 2 deviates from Stage 1 (1/20). This suggests that the initial condition of quanta/excess CO_2 shouldn't be ignored in C_t derivation when infection ratio varies among occupancy stages. As the infection ratio for case 1 changes (either increase or decrease from 1/20 in Stage 1), the derived C_t for Stage 2 in case 1 will be larger or smaller, respectively, compared to the derived C_t for Stage 2 in case 2. The difference between the two cases becomes more pronounced as the infection ratio of case 1 deviates further from 1/20. When the infection ratio increases from 1/20 (Stage 1) to 1/5 (Stage 2), C_{t50} of case 1 with initial quanta/excess CO_2 increases by 60 ppm compared to case 2 without initial quanta/excess CO_2. Conversely, when the infection ratio decreases from 1/20 to 1/80 in Stage 2, C_{t50} of case 1 becomes 260 ppm lower.

4. Discussion

4.1. New understanding of rebreathed-fraction model

RF-based Wells-Riley model, proposed by Rudnick and Milton's [14], uses CO_2 as a maker for exhaled-breath exposure. This model does not require any knowledge about ACH, hence it has been widely used in assessing airborne infection risk [42–46]. However, we proved that RF-based model should only be adopted in spaces with fixed occupancy, otherwise initial quanta will cause bias (see Part 3.3), which is largely overlooked by many other studies. For spaces with varying occupancy, the initial quanta/excess CO_2 generated by previous occupants but remaining in the air can be very important in determining the overall quanta/excess CO_2 concentration for next-stage occupancy. The mechanism of RF-based model in dealing with initial quanta/excess CO_2 in spaces with changing occupancy has not been adequately discussed before. In this article, we provide an analytical derivation to explain its mechanism and show that initial quanta/excess CO_2 can be considered within the RF-based method in C_t derivation for Scenario 1 (with fixed occupancy) and Scenario 2 (with changing occupancy but fixed infection ratios). This extends the generalization of RF-based model from spaces with fixed occupancy to spaces with changing occupancy. It should be noted that other recent studies [28,29] resonate with our study in that they apply RF-based model to spaces with varying occupancy levels to assess infection risk. However, only two occupancy modes were considered in these studies, occupied and non-occupied, which are both included in our Scenario 1. In this contribution, we have proved that for spaces with both occupied and non-occupied modes, the non-occupied period does not affect the proportion of quanta concentration to excess CO_2 concentration in future occupied period if infection ratios remain unchanged given only ventilation is considered here (see Supplementary Information).

4.2. Implications for C_t determination

Great uncertainty in C_t can be caused by the uncertainties in emissions of E_q and E_{CO2} (see Fig. 1). E_{CO2} and E_q contain uncertainty because they have interindividual variation and can be affected by factors such as age, gender [16–18]. The value of E_q can vary by up to 3 orders of magnitude (e.g., 0.32–240 quanta/h for speaking under light activity) [16] while E_{CO2} varies within only one order of magnitude (e.g., 2.88–43.2 L/h) [17]. Different studies adopted very different values of E_q and therefore lead to very different values of C_t. For example, in the classroom setting under the same activity level, the median value of E_q in our study is 0.37 quanta/h [16], while it was in the range of 27.55 quanta/h to 100 quanta/h in other studies [6,13,22], leading several hundred times lower C_t compared to our results.

The choices of P_t and I_i also impact the value of C_t. Theoretically, a lower P_t can promise a safer indoor environment, but this would come at the cost of very low C_t practically impossible to achieve in real-world scenarios. E.g., a low level of C_t may require a very high ACH, which is unfeasible and prone to cause large energy cost due to the diminishing return phenomenon of ventilation [47]. Additionally, the method to determine infector number I_i is also important, as it is related to the total quanta emission. Our study defined I_i as the maximum value of $\{1, P_I N_i\}$ as the worst-case scenario. On the contrary, Bazant et al. [22] considered I_i to be the minimum value of $\{1, P_I N_i\}$, which resulted in a dramatically large value of C_t (even larger than 10000 ppm) when P_I is small.

4.3. Implications for infection risk monitoring and control

Our model has practical implications for indoor transmission monitoring and control. For Scenario 1 and Scenario 2, the safe excess CO_2 threshold can be determined based on variables such as occupancy level, duration and risk threshold through simple equations (see Equation (9) and Equation (12)), making it possible to apply our model for infection risk monitoring in Scenario 1 and 2 for public individuals. For instance, when entering a space like as a shopping center (as in our Scenario 2), individuals can easily measure the indoor excess CO_2 level first using a portable low-cost CO_2 sensor. Then, by replacing C_t in Equation (12) with the measured data, they can estimate a safe exposure duration based on their acceptable risk threshold to guide them on how long they should stay in the shopping center. Additionally, taking into account the impact of initial quanta/excess CO_2 on risk estimation and C_t derivation, our model can be adopted to further develop different ventilation control strategies, such as CO_2-based demand-controlled ventilation [48] or intermittent ventilation strategy [49,50], aimed at reducing indoor

transmission risk by treating indoor excess CO_2 as a control variable.

Further applying our calculation framework into real-world scenarios, some insights can be gained by comparing derived C_t with measurement data/standard limits. In Scenario 1, the occupant numbers can largely affect C_t level, making it necessary to consider both CO_2 level and occupant level in transmission risk assessment. For example, in classrooms of Scenario 1, the measured excess CO_2 levels were found to be in the range of 300–2500 ppm (with an outdoor level of 420 ppm) dependent on the number of occupants [7,29,51]. According to our framework, 300 ppm can represent an unsafe environment if the occupant number is less than 33, and 2500 ppm can still be a safe level if occupants is larger than 278. Therefore, C_t threshold should be used in conjunction with occupant number. In scenario 2, community prevalence can dominate C_t and can be used as a reference for lockdown policy implementation. It was found that the 1-h average CO_2 level of 40% shopping mall in Hong Kong exceeded 1000 ppm [52]. To keep infection risk no more than 0.01% for shopping malls, a community prevalence of less than 0.09% is needed according to our calculation framework, otherwise, such places should be locked down. In Scenario 3, taking a restaurant (~350 m^3) with two occupancy stage ($N_1 = 20$ for Stage 1 and $N_2 = 80$ for Stage 2) as an example [53], according to ASHRAE 62.1 [54], the maximum excess CO_2 limits (the steady-state excess CO_2 concentration under the required ventilation rate) for the first two occupancy stages are 540 ppm (Stage 1) and 790 ppm (Stage 2) respectively. But C_t calculated from our framework amounts to 180 ppm and 610 ppm, respectively. The difference indicates the target of infection risk control should be integrated into present ventilation standards to promise both a high level of IAQ and a low infection risk.

4.4. Limitation of the study

Our study is based on the assumption that outdoor ventilation is the only loss mechanism for quanta in Scenario 1 and Scenario 2, which results in a constant proportion between quanta concentration and excess CO_2 concentration, hence making RF-based model suitable for deriving C_t in these scenarios. However, surface deposition, filtration and virus deactivation can also significantly reduce quanta concentration [55–57]. Neglecting these loss mechanisms may overestimate indoor quanta concentration and result in a lower C_t than needed. However, the reliability of the derived C_t for a safe indoor environment would not be affected.

The thresholds we derived are based on the assumption of a well-mixed room air. Thus, the location of CO_2 sensors need to be carefully selected to adequately reflect indoor CO_2 conditions [58,59]. Additionally, our results only account for long-range airborne transmission neglecting the contribution of short-range transmission [4,37,60]. Relying solely on C_t to monitor infection risk may not be sufficient, other measures such as wearing masks and social distancing should be implemented together to control indoor airborne transmission [61–63].

Another limitation lies in the application of community prevalence (P_I) in our study. In scenario 1 and scenario 3, P_I is used to determine the indoor infector number, which would cause bias because: 1) P_I might be lower than the real value due to the asymptomatic characteristic of SARS-CoV-2 [64,65]; and 2) positive individuals may not be present in public spaces due to mandatory quarantine policy which would lead to a lower indoor infection ratio than P_I. In scenario 2, simply using P_I to represent the indoor infection ratio can lead to an underestimation of the actual ratio when the number of occupants is low. Conducting field measurement to estimate the average occupancy level (N_{ave}) and selecting the maximum value of $\{1, P_I N_{ave}\}$ could be an alternative method for defining a convincible infection ratio for scenario 2. In addition, considering P_I is changing during different time periods of pandemic, the indoor infection ratio would need to be updated accordingly.

In addition, the uncertainty of C_t estimated by our study may be limited as we only considered the uncertainty in emission settings (i.e., quanta emission rate, CO_2 emission rate). Community prevalence (P_I) may also contain uncertainty due to the reasons described earlier. This uncertainty may increase the uncertainty of C_t for Scenario 2, where P_I is a dominating input in C_t derivation. However, it may not obviously affect C_t for Scenario 1 and 3, because P_I is only adopted in C_t derivation when $P_I N_i > 1$ but the occupancy level (N_i) in Scenario 1 and 3 is usually low and hence $P_I N_i < 1$. Similar as emission settings, breathing rate can also contain uncertainty due to interindividual variation and factors such as age and gender. In addition, quanta emission rate, CO_2 emission rate and breathing rate may all be correlated to each other [18]. In our study, we simply adopted constant breathing rates for different physical activity levels based on the study of Buonanno et al. [16]. Quanta emission rate and CO_2 emission rate are also inter-related through physical activity level (See Table 1). In future, based on more accurate data, the uncertainty and correlation of those parameters may be better interpreted, and the uncertainty of C_t can be therefore further estimated.

5. Conclusion

A new calculation framework was proposed in this study for deriving safe excess CO_2 threshold (C_t) for different spaces with consideration of initial quanta/excess CO_2 and fixed/changing occupancy levels. From our derivation process we found that the proportion of indoor excess CO_2 concentration to quanta concentration remains constant when the infection ratio (infectors/occupants) of an indoor space remains constant. Based on this relationship, the RF-based (rebreathed fraction-based) model can be applied directly for infection risk assessment and C_t derivation, but not applicable in the cases with varying infection ratios.

Affected by factors such as occupant number (N_i), community prevalence (P_I) and activity level, the median value C_{t50} derived by our framework varies significantly among the selected cases, with a minimum value of 7 ppm for a gym to a maximum value of 890 ppm for a lecture hall, with long-tailed distributions. Initial quanta/excess CO_2 is found to largely affect C_t, especially when the infection ratio varies greatly during different occupancy stages. A bias of several hundred ppm (e.g., 260 ppm for a space of 300 m^3 and with sedentary activity level) could be occur if the initial quanta is not well considered in C_t derivation. Our finding illustrates that different CO_2 thresholds should be derived for different spaces and different occupancy stages, rather than using a fixed value for all spaces.

Large uncertainty was also found in derived thresholds for all cases, spanning approximately 6 orders of magnitude, mainly influenced by quanta emission rate (E_q) and CO_2 emission rate (E_{CO2}). For a better control of indoor infection risk through CO_2 monitoring, more accurate input parameters would be necessary.

CRediT authorship contribution statement

Xiaowei Lyu: Writing – review & editing, Writing – original draft, Visualization, Methodology, Investigation, Formal analysis, Data curation, Conceptualization. **Zhiwen Luo:** Writing – review & editing, Writing – original draft, Supervision, Resources, Project administration, Methodology, Investigation, Funding acquisition, Conceptualization. **Li Shao:** Writing – review & editing, Supervision, Investigation. **Hazim Awbi:** Writing – review & editing, Investigation. **Samuele Lo Piano:** Writing – review & editing, Methodology.

Declaration of competing interest

The authors declare the following financial interests/personal relationships which may be considered as potential competing interests: Xiaowei Lyu reports financial support was provided by China Scholarship Council.

Data availability

Data will be made available on request.

Acknowledgement

XL acknowledged the financial support from China Scholarship Council (CSC) for pursuing her PhD at the University of Reading, UK.

Appendix A. Supplementary data

Supplementary data to this article can be found online at https://doi.org/10.1016/j.buildenv.2022.109967.

References

[1] N. Chen, M. Zhou, X. Dong, J. Qu, F. Gong, Y. Han, Y. Qiu, J. Wang, Y. Liu, Y. Wei, J. Xia, T. Yu, X. Zhang, L. Zhang, Epidemiological and clinical characteristics of 99 cases of 2019 novel coronavirus pneumonia in Wuhan, China: a descriptive study, Lancet 395 (2020) 507–513, https://doi.org/10.1016/S0140-6736(20)30211-7.

[2] H. Qian, T. Miao, L. Liu, X. Zheng, D. Luo, Y. Li, Indoor transmission of SARS-CoV-2, Indoor Air 31 (2021) 639–645, https://doi.org/10.1111/ina.12766.

[3] J. Wei, Y. Li, Airborne spread of infectious agents in the indoor environment, Am. J. Infect. Control 44 (2016), https://doi.org/10.1016/j.ajic.2016.06.003. S102–S108.

[4] Y. Li, Basic routes of transmission of respiratory pathogens—a new proposal for transmission categorization based on respiratory spray, inhalation, and touch, Indoor Air 31 (2021) 3–6, https://doi.org/10.1111/ina.12786.

[5] Z. Peng, A.L.P. Rojas, E. Kropff, W. Bahnfleth, G. Buonanno, S.J. Dancer, J. Kurnitski, Y. Li, M.G.L.C. Loomans, L.C. Marr, L. Morawska, W. Nazaroff, C. Noakes, X. Querol, C. Sekhar, R. Tellier, T. Greenhalgh, L. Bourouiba, A. Boerstra, J.W. Tang, S.L. Miller, J.L. Jimenez, Practical indicators for risk of airborne transmission in shared indoor environments and their application to COVID-19 outbreaks, Environ. Sci. Technol. 56 (2022) 1125–1137, https://doi.org/10.1021/acs.est.1c06531.

[6] Z. Peng, J.L. Jimenez, Exhaled CO2as a COVID-19 infection risk proxy for different indoor environments and activities, Environ. Sci. Technol. Lett. 8 (2021) 392–397, https://doi.org/10.1021/acs.estlett.1c00183.

[7] A. Persily, W.P. Bahnfleth, H. Kipen, J. Lau, C. Mandin, C. Sekhar, P. Wargocki, L. C. Nguyen Weekes, ASHRAE Position Document on Indoor Carbon Dioxide, ASHRAE J, 2022, pp. 50–52. https://tsapps.nist.gov/publication/get_pdf.cfm?pub_id=934476. (Accessed 4 October 2022).

[8] REHVA, REHVA COVID19 GUIDANCE Version 4.1, 2021. https://www.rehva.eu/fileadmin/user_upload/REHVA_COVID-19_guidance_document_V4.1_150420 21.pdf. (Accessed 3 October 2022).

[9] SAGE-EMG, EMG-SPI-B: Application of CO2 Monitoring as an Approach to Managing Ventilation to Mitigate SARS-CoV-2 Transmission, 2021. https://www.gov.uk/government/publications/emg-role-of-ventilation-in-controllingsars-cov-2-transmission-30-september-2020. (Accessed 3 October 2022).

[10] CIBSE, COVID-19: Ventilation, 2021. https://www.cibse.org/Coronavirus-COVID-19. (Accessed 4 October 2022).

[11] CDC, Ventilation in Buildings, 2021. https://www.cdc.gov/coronavirus/2019-ncov/community/ventilation.html. (Accessed 14 October 2022).

[12] SAGE-EMG, Role of Ventilation in Controlling SARS-CoV-2 Transmission, SAGE-EMG, 2020. https://www.gov.uk/government/publications/emg-role-of-ventilation-in-controllingsars-cov-2-transmission-30-september-2020. (Accessed 3 October 2022).

[13] D. Hou, A. Katal, L. Leon, Wang, A. Katal1, L. Leon, Wang, Bayesian Calibration of Using CO2 Sensors to Assess Ventilation Conditions and Associated COVID-19 Airborne Aerosol Transmission Risk in Schools, MedRxiv, 2021, 2021.01.29.21250791, http://medrxiv.org/content/early/2021/02/03/2021.01.29.21250791.abstract.

[14] S.N. Rudnick, D.K. Milton, Risk of Indoor Airborne Infection Transmission Estimated from Carbon Dioxide Concentration, 2003. www.blackwellpublishing.com/ina.

[15] R. Mittal, R. Ni, J.H. Seo, The flow physics of COVID-19, J. Fluid Mech. 894 (2020), https://doi.org/10.1017/jfm.2020.330.

[16] G. Buonanno, L. Morawska, L. Stabile, Quantitative assessment of the risk of airborne transmission of SARS-CoV-2 infection : prospective and retrospective applications, Environ. Int. 145 (2020), 106112, https://doi.org/10.1016/j.envint.2020.106112.

[17] A. Persily, L. de Jonge, Carbon dioxide generation rates for building occupants, Indoor Air 27 (2017) 868–879, https://doi.org/10.1111/ina.12383.

[18] N. Good, K.M. Fedak, D. Goble, A. Keisling, C. L'Orange, E. Morton, R. Phillips, K. Tanner, J. Volckens, Respiratory aerosol emissions from vocalization: age and sex differences are explained by volume and exhaled CO2, Environ. Sci. Technol. Lett. 8 (2021) 1071–1076, https://doi.org/10.1021/acs.estlett.1c00760.

[19] J. Lelieveld, F. Helleis, S. Borrmann, Y. Cheng, F. Drewnick, G. Haug, T. Klimach, J. Sciare, H. Su, U. Pöschl, Model calculations of aerosol transmission and infection risk of covid-19 in indoor environments, Int. J. Environ. Res. Publ. Health 17 (2020) 1–18, https://doi.org/10.3390/ijerph17218114.

[20] R. Ke, C. Zitzmann, D.D. Ho, R.M. Ribeiro, A.S. Perelson, In vivo kinetics of SARS-CoV-2 infection and its relationship with a person's infectiousness, Proc. Natl. Acad. Sci. U. S. A. 118 (2021), https://doi.org/10.1073/pnas.2111477118/-/DCSupplemental.

[21] R. Ke, P.P. Martinez, R.L. Smith, L.L. Gibson, A. Mirza, M. Conte, N. Gallagher, C. H. Luo, J. Jarrett, R. Zhou, A. Conte, T. Liu, M. Farjo, K.K.O. Walden, G. Rendon, C. J. Fields, L. Wang, R. Fredrickson, D.C. Edmonson, M.E. Baughman, K.K. Chiu, H. Choi, K.R. Scardina, S. Bradley, S.L. Gloss, C. Reinhart, J. Yedetore, J. Quicksall, A.N. Owens, J. Broach, B. Barton, P. Lazar, W.J. Heetderks, M.L. Robinson, H. H. Mostafa, Y.C. Manabe, A. Pekosz, D.D. McManus, C.B. Brooke, Daily longitudinal sampling of SARS-CoV-2 infection reveals substantial heterogeneity in infectiousness, Nat Microbiol 7 (2022) 640–652, https://doi.org/10.1038/s41564-022-01105-z.

[22] M.Z. Bazant, O. Kodio, A.E. Cohen, K. Khan, Z. Gu, J.W.M. Bush, Monitoring carbon dioxide to quantify the risk of indoor airborne transmission of COVID-19, Flowline 1 (2021) 1–17, https://doi.org/10.1017/flo.2021.10.

[23] E.C. Riley, G. Murphy, R.L. Riley, Airborne spread of measles in a suburban elementary school, Am. J. Epidemiol. 107 (1978), https://doi.org/10.1093/oxfordjournals.aje.a112560.

[24] L. Gammaitoni, M.C. Nucci, Using a mathematical model to evaluate the efficacy of TB control measures, Emerg. Infect. Dis. 3 (1997), https://doi.org/10.3201/eid0303.970310.

[25] H. Dai, B. Zhao, Association of the infection probability of COVID-19 with ventilation rates in confined spaces, Build. Simulat. 13 (2020) 1321–1327, https://doi.org/10.1007/s12273-020-0703-5.

[26] Y. Ma, C.R. Horsburgh, L.F. White, H.E. Jenkins, Quantifying TB transmission: a systematic review of reproduction number and serial interval estimates for tuberculosis, Epidemiol. Infect. 146 (2018) 1478–1494, https://doi.org/10.1017/S0950268818001760.

[27] H. Furuya, M. Nagamine, T. Watanabe, Use of a mathematical model to estimate tuberculosis transmission risk in an Internet café, Environ. Health Prev. Med. 14 (2009) 96–102, https://doi.org/10.1007/s12199-008-0062-9.

[28] H.C. Burridge, S. Fan, R.L. Jones, C.J. Noakes, P.F. Linden, Predictive and Retrospective Modelling of Airborne Infection Risk Using Monitored Carbon Dioxide, Indoor and Built Environment, 2021, https://doi.org/10.1177/1420326x211043564, 1420326X2110435.

[29] C.V.M. Vouriot, H.C. Burridge, C.J. Noakes, P.F. Linden, Seasonal variation in airborne infection risk in schools due to changes in ventilation inferred from monitored carbon dioxide, Indoor Air 31 (2021) 1154–1163, https://doi.org/10.1111/ina.12818.

[30] M. Mihi, I.-D. Ani, M. Mihi, F. Professor, I. Ani, I. Kursan Milaković, A. Professor, Time Spent Shopping and Consumer Clothing Purchasing Behaviour EKONOMSKI PREGLED, 2018.

[31] C. Molina, B. Jones, Investigating Uncertainty in the Relationship between Indoor Steady-State CO2 Concentrations and Ventilation Rates, Aivc, 2021, https://doi.org/10.13140/RG.2.2.16867.99361.

[32] B.E. Ainsworth, W.L. Haskell, M.C. Whitt, M.L. Irwin, A.M. Swartz, S.J. Strath, W. L. O'Brien, J. Bassett, K.H. Schmitz, P.O. Emplaincourt, J. Jacobs, A.S. Leon, Compendium of physical activities: an update of activity codes and MET intensities, Med. Sci. Sports Exerc. 32 (2000), https://doi.org/10.1097/00005768-200009001-00009.

[33] K.-T. Fang, R. Li, A. Sudjianto, Design and Modeling for Computer Experiments, Chapman and Hall/CRC, 2005, https://doi.org/10.1201/9781420034899.

[34] I.M. Sobol', A Primer for the Monte Carlo Method, CRC Press, 2018, https://doi.org/10.1201/9781315136448.

[35] K.B. Pouwels, T. House, E. Pritchard, J.v. Robotham, P.J. Birrell, A. Gelman, K. D. Vihta, N. Bowers, I. Boreham, H. Thomas, J. Lewis, I. Bell, J.I. Bell, J.N. Newton, J. Farrar, I. Diamond, P. Benton, A.S. Walker, K.B. Pouwels, A.S. Walker, D. Crook, P.C. Matthews, T. Peto, N. Stoesser, A. Howarth, G. Doherty, J. Kavanagh, K. K. Chau, S.B. Hatch, D. Ebner, L. Martins Ferreira, T. Christott, B.D. Marsden, W. Dejnirattisai, J. Mongkolsapaya, S. Hoosdally, R. Cornall, D.I. Stuart, G. Screaton, D. Eyre, J. Bell, S. Cox, K. Paddon, T. James, J.N. Newton, J. v. Robotham, P. Birrell, H. Jordan, T. Sheppard, G. Athey, D. Moody, L. Curry, P. Brereton, J. Hay, H. Vansteenhouse, A. Lambert, E. Rourke, S. Hawkes, S. Henry, J. Scruton, P. Stokes, T. Thomas, J. Allen, R. Black, H. Bovill, D. Braunholtz, D. Brown, S. Collyer, M. Crees, C. Daglish, B. Davies, H. Donnarumma, J. Douglas-Mann, A. Felton, H. Finselbach, E. Fordham, A. Ipser, J. Jenkins, J. Jones, K. Kent, G. Kerai, L. Lloyd, V. Masding, E. Osborn, A. Patel, E. Pereira, T. Pett, M. Randall, D. Reeve, P. Shah, R. Snook, R. Studley, E. Sutherland, E. Swinn, A. Tudor, J. Weston, S. Leib, J. Tierney, G. Farkas, R. Cobb, F. van Galen, L. Compton, J. Irving, J. Clarke, R. Mullis, L. Ireland, D. Airimitoaie, C. Nash, D. Cox, S. Fisher, Z. Moore, J. McLean, M. Kerby, Community prevalence of SARS-CoV-2 in england from april to november, 2020: results from the ONS coronavirus infection survey, Lancet Public Health 6 (2021) e30–e38, https://doi.org/10.1016/S2468-2667(20)30282-6.

[36] Adam, Measurement of Breathing Rate and Volume in Routinely Performed Daily Activities, 1993.

[37] W. Chen, H. Qian, N. Zhang, F. Liu, L. Liu, Y. Li, Extended short-range airborne transmission of respiratory infections, J. Hazard Mater. 422 (2022), https://doi.org/10.1016/j.jhazmat.2021.126837.

[38] W. Jia, J. Wei, P. Cheng, Q. Wang, Y. Li, Exposure and respiratory infection risk via the short-range airborne route, Build. Environ. 219 (2022), https://doi.org/10.1016/j.buildenv.2022.109166.

[39] B. Jones, P. Sharpe, C. Iddon, E.A. Hathway, C.J. Noakes, S. Fitzgerald, Modelling uncertainty in the relative risk of exposure to the SARS-CoV-2 virus by airborne

aerosol transmission in well mixed indoor air, Build. Environ. 191 (2021), https://doi.org/10.1016/j.buildenv.2021.107617.
[40] G. Buonanno, L. Stabile, L. Morawska, Estimation of airborne viral emission : quanta emission rate of SARS-CoV-2 for infection risk assessment, Environ. Int. 141 (2020), 105794, https://doi.org/10.1016/j.envint.2020.105794.
[41] S. Zhang, Z. Lin, Dilution-based evaluation of airborne infection risk - thorough expansion of Wells-Riley model, Build. Environ. 194 (2021), https://doi.org/10.1016/j.buildenv.2021.107674.
[42] J.R. Andrews, C. Morrow, R.P. Walensky, R. Wood, Integrating social contact and environmental data in evaluating tuberculosis transmission in a South African township, JID (J. Infect. Dis.) 210 (2014) 597–603, https://doi.org/10.1093/infdis/jiu138.
[43] J. Hella, C. Morrow, F. Mhimbira, S. Ginsberg, N. Chitnis, S. Gagneux, B. Mutayoba, R. Wood, L. Fenner, Tuberculosis transmission in public locations in Tanzania: a novel approach to studying airborne disease transmission, J. Infect. 75 (2017) 191–197, https://doi.org/10.1016/j.jinf.2017.06.009.
[44] E.T. Richardson, C.D. Morrow, D.B. Kalil, L.G. Bekker, R. Wood, Shared air: a renewed focus on ventilation for the prevention of tuberculosis transmission, PLoS One 9 (2014) 1–7, https://doi.org/10.1371/journal.pone.0096334.
[45] R. Wood, C. Morrow, S. Ginsberg, E. Piccoli, D. Kalil, A. Sassi, R.P. Walensky, J. R. Andrews, Quantification of shared air: a Social and environmental determinant of airborne disease transmission, PLoS One 9 (2014) 1–8, https://doi.org/10.1371/journal.pone.0106622.
[46] K. Zürcher, C. Morrow, J. Riou, M. Ballif, A.S. Koch, S. Bertschinger, X. Liu, M. Sharma, K. Middelkoop, D. Warner, R. Wood, M. Egger, L. Fenner, Novel approach to estimate tuberculosis transmission in primary care clinics in sub-Saharan Africa: protocol of a prospective study, BMJ Open 10 (2020), https://doi.org/10.1136/bmjopen-2019-036214.
[47] Y. Li, P. Cheng, W. Jia, Poor ventilation worsens short-range airborne transmission of respiratory infection, Indoor Air (2021), https://doi.org/10.1111/ina.12946.
[48] B. Li, W. Cai, A novel CO2-based demand-controlled ventilation strategy to limit the spread of COVID-19 in the indoor environment, Build. Environ. 219 (2022), https://doi.org/10.1016/j.buildenv.2022.109232.
[49] A.K. Melikov, Z.T. Ai, D.G. Markov, Intermittent occupancy combined with ventilation: an efficient strategy for the reduction of airborne transmission indoors, Sci. Total Environ. (2020) 744, https://doi.org/10.1016/j.scitotenv.2020.140908.
[50] S. Zhang, D. Niu, Z. Lin, Occupancy-aided Ventilation for Airborne Infection Risk Control: Continuously or Intermittently Reduced Occupancies? Build Simul, 2022 https://doi.org/10.1007/s12273-022-0951-7.
[51] Z. Bakó-Biró, D.J. Clements-Croome, N. Kochhar, H.B. Awbi, M.J. Williams, Ventilation rates in schools and pupils' performance, Build. Environ. 48 (2012) 215–223, https://doi.org/10.1016/j.buildenv.2011.08.018.
[52] W.M. Li, S.C. Lee, L.Y. Chan, Indoor air quality at nine shopping malls in Hong Kong, Sci. Total Environ. 273 (2001) 27–40, https://doi.org/10.1016/S0048-9697(00)00833-0.
[53] J. Shen, M. Kong, B. Dong, M.J. Birnkrant, J. Zhang, A systematic approach to estimating the effectiveness of multi-scale IAQ strategies for reducing the risk of airborne infection of SARS-CoV-2, Build. Environ. 200 (2021), https://doi.org/10.1016/j.buildenv.2021.107926.
[54] ASHRAE, ANSI/ASHRAE Standard 62.1-2019, Ventilation for Acceptable Indoor Airquality, 2019.
[55] B. Blocken, T. van Druenen, A. Ricci, L. Kang, T. van Hooff, P. Qin, L. Xia, C. A. Ruiz, J.H. Arts, J.F.L. Diepens, G.A. Maas, S.G. Gillmeier, S.B. Vos, A. C. Brombacher, Ventilation and air cleaning to limit aerosol particle concentrations in a gym during the COVID-19 pandemic, Build. Environ. 193 (2021), https://doi.org/10.1016/j.buildenv.2021.107659.
[56] A. Su, S.M. Grist, A. Geldert, A. Gopal, A.E. Herr, Quantitative UV-C dose validation with photochromic indicators for informed N95 emergency decontamination, PLoS One 16 (2021), https://doi.org/10.1371/journal.pone.0243554.
[57] N. van Doremalen, T. Bushmaker, D.H. Morris, M.G. Holbrook, A. Gamble, B. N. Williamson, A. Tamin, J.L. Harcourt, N.J. Thornburg, S.I. Gerber, J.O. Lloyd-Smith, E. de Wit, V.J. Munster, Aerosol and surface stability of SARS-CoV-2 as compared with SARS-CoV-1, N. Engl. J. Med. 382 (2020) 1564–1567, https://doi.org/10.1056/nejmc2004973.
[58] N. Mahyuddin, H. Awbi, The spatial distribution of carbon dioxide in an environmental test chamber, Build. Environ. 45 (2010) 1993–2001, https://doi.org/10.1016/j.buildenv.2010.02.001.
[59] N. Mahyuddin, H.B. Awbi, M. Alshitawi, The spatial distribution of carbon dioxide in rooms with particular application to classrooms, Indoor Built Environ. 23 (2014) 433–448, https://doi.org/10.1177/1420326X13512142.
[60] C.X. Gao, Y. Li, J. Wei, S. Cotton, M. Hamilton, L. Wang, B.J. Cowling, Multi-route respiratory infection: when a transmission route may dominate, Sci. Total Environ. 752 (2021), 141856, https://doi.org/10.1016/j.scitotenv.2020.141856.
[61] M.C. Jarvis, Aerosol transmission of SARS-CoV-2: physical principles and implications, Front. Public Health 8 (2020), https://doi.org/10.3389/fpubh.2020.590041.
[62] R. Mittal, C. Meneveau, W. Wu, A mathematical framework for estimating risk of airborne transmission of COVID-19 with application to face mask use and social distancing, Phys. Fluids 32 (2020), https://doi.org/10.1063/5.0025476.
[63] J. Wagner, T.L. Sparks, S. Miller, W. Chen, J.M. Macher, J.M. Waldman, Modeling the impacts of physical distancing and other exposure determinants on aerosol transmission, J. Occup. Environ. Hyg. (2021) 1–15, https://doi.org/10.1080/15459624.2021.1963445.
[64] S. Lee, T. Kim, E. Lee, C. Lee, H. Kim, H. Rhee, S.Y. Park, H.J. Son, S. Yu, J.W. Park, E.J. Choo, S. Park, M. Loeb, T.H. Kim, Clinical course and molecular viral shedding among asymptomatic and symptomatic patients with SARS-CoV-2 infection in a community treatment center in the Republic of Korea, JAMA Intern. Med. 180 (2020) 1447–1452, https://doi.org/10.1001/jamainternmed.2020.3862.
[65] A.M. Pollock, J. Lancaster, Asymptomatic transmission of covid-19, BMJ (2020) 371, https://doi.org/10.1136/bmj.m4851.